Atmospheric Environment 168 (2017) 112–124

Contents lists available at ScienceDirect

Atmospheric Environment

journal homepage: www.elsevier.com/locate/atmosenv

Influence of synoptic condition and holiday effects on VOCs and ozone production in the Yangtze River Delta region, China

Zhengning Xu [a, b], Xin Huang [a, b, *], Wei Nie [a, b], Xuguang Chi [a, b], Zheng Xu [a, b], Longfei Zheng [a, b], Peng Sun [a, b], Aijun Ding [a, b]

[a] Joint International Research Laboratory of Atmospheric and Earth System Sciences, School of Atmospheric Sciences, Nanjing University, 210023, Nanjing, China

[b] Collaborative Innovation Center of Climate Change, Jiangsu Province, China

ARTICLE INFO

Article history:
Received 19 April 2017
Received in revised form
11 August 2017
Accepted 14 August 2017
Available online 15 August 2017

Keywords:
Volatile organic compounds
Ozone formation
Yangtze River Delta region
Holiday effect
Synoptic condition

ABSTRACT

Both anthropogenic emission and synoptic conditions play important roles in ozone (O_3) formation and accumulation. In order to understand the influence of synoptic condition and holiday effects on ozone production in the Yangtze River Delta region, China, concentrations of speciated volatile organic compounds (VOCs) and O_3 as well as other relevant trace gases were simultaneously measured at the Station for Observing Regional Processes of the Earth System (SORPES) in Nanjing around the National Day holidays of China in 2014, which featured substantial change of emissions and dominated by typical anti-cyclones. Different groups of VOC species and their chemical reactivities were comprehensively analyzed. We observed clear diurnal variations of short alkenes during the measurement period, considerable amount of short alkenes were observed during night (more than 10 ppb) while almost no alkenes were measured during daytime, which might be attributed to different chemical processes. The obvious enhancement of the VOC tracers during the National Day holidays (Oct. 1st-Oct. 7th) indicated that the holiday effect strongly influenced the distribution of VOC profile and chemical reactivity in the atmosphere. At the same time, two meso-scale anticyclone processes were also observed during the measurement period. The synoptic condition contributed to the accumulation of VOCs and other precursors, which consequently impacted the ozone production in this region. The integrated influence of synoptic and holiday effects was also analyzed with an Observation Based Model (OBM) based on simplified MCM (Master Chemical Mechanism) chemical mechanism. The calculated relative increment reactivity (RIR) of different VOC groups revealed that during the holidays, this region was in VOC-limited regime and the variation of RIR shows a close linkage to the development and elimination of anti-cyclones, indicating an in-negligible contribution of synoptic effect toward ozone production in this region.

1. Introduction

Ozone (O_3), one of the major components of photochemical pollutants in the troposphere, jeopardizes human immune system, nerve system as well as respiratory system (Brunekreef and Holgate, 2002). It also affects, negatively, the crop yield and forest growth (Fuhrer et al., 1997). Moreover, ozone is one of the major greenhouse gases influencing climate change on global scale (Seinfeld and Pandis, 2006; IPCC, 2013). The photochemical reactions of volatile organic compounds (VOCs) and nitrogen oxides (NO_x) are the main sources of tropospheric ozone (Chameides, 1992; Atkinson, 1998; Arey and Atkinson, 2003).

Intensive anthropogenic VOCs and NO_x emissions and their variations directly connect with ozone formation rate in urban and semi-urban areas (Zhang et al., 2008; Guo et al., 2009). It is a widespread phenomenon that, during holiday or weekend, daytime surface ozone concentrations in urban areas tend to have different variation pattern compared with normal days. Studies about holiday effects from Chinese New Year indicated a negative impact on the air quality. Ozone concentration in Taiwan was higher than normal days at every hour of the diurnal cycle (Tan et al., 2009,

* Corresponding author. Joint International Research Laboratory of Atmospheric and Earth System Sciences, School of Atmospheric Sciences, Nanjing University, 210023, Nanjing, China.
E-mail address: xinhuang@nju.edu.cn (X. Huang).

http://dx.doi.org/10.1016/j.atmosenv.2017.08.035

2013), while the short-term effects of the Jewish holiday of Day of Atonement in Israel led to a dramatic decrease of primary pollution such as NO and a minor increase of ozone (Levy, 2013). The weekend effects on near-surface ozone concentration were also studied in Switzerland. Under favorable meteorological conditions, the peak ozone concentration could reduce 10–15%, compared with weekdays (Brönnimann and Neu, 1997). It has been proved that decreased concentrations of NO_x emissions from on-road motor vehicles during holiday or weekend is a dominant cause of increased/decreased ozone concentrations (Pollack et al., 2012).

In addition to the fluctuation in the intensity of anthropogenic activities, synoptic conditions also play an important role in the transport and accumulation of ozone and its precursors (Wang et al., 2009; Zhang et al., 2013; Ding et al., 2017a). For example, an approaching Northwest Pacific Typhoon often caused delayed sea-land breezes and the low mixing height in the Pearl River Delta region in South China, resulting in the accumulation of primary pollutants and ozone production along the coastal city clusters (Ding et al., 2004; Wei et al., 2016). Warm conveyer belts and the fronts would promote long-range transport by lifting surface pollutants to free troposphere (Ding et al., 2009). The variations of ozone in eastern China were strongly influenced by the evolution of synoptic weather (Jiang et al., 2012; Ding et al., 2013a).

The Yangtze River Delta (YRD) region, one of the most economically developed regions in eastern China, has been suffering from severe air pollution in past decades. Satellite observation of NO_2 column concentration from 2000 to 2008 has showed that the YRD region is one of the most polluted city clusters in China (Huang et al., 2011). As the consequences of fast development and population explosion, anthropogenic emission, including vehicle and residential activities, power plants, and industrial productions (iron and steel manufacturing, oil refinery, and solvent usage), have increased dramatically (Liu et al., 2008a). The emission estimation of the YRD region indicates that the emissions concentrate in the urban and industrial areas along the Yangtze River and around Hangzhou Bay (Li et al., 2016). Continuous measurements of ozone in the western YRD region have pointed out an increasing trend of ozone concentration, while the nitrogen oxides kept decreasing in past few years (Ding et al., 2017b). Consequently, it is of great interest and necessity to investigate the current relations between ozone and its precursors in the YRD region from both perspectives of air pollution policy making and scientific purposes. Existing numerical studies on the ozone formation in the YRD region were mainly based on three dimensional chemical transport model (CTM), while most observational studies in this region usually utilize CO as the proxy of VOCs to assess the role of VOCs and their role in ozone formation (Ding et al., 2013a; Xie et al., 2016). One shortcoming is that it is not capable of quantifying the contribution of VOCs in ozone formation. Additionally, the spatio-temporal pattern of CO generally differs from those of VOCs and different kinds of VOCs features disparities in reactivity (Arey and Atkinson, 2003; Shao et al., 2009). A combination of in-situ measurement and theoretical calculation would shed more light on ozone formation (Xue et al., 2013a, 2013b, 2014). However, in the YRD region few studies about the ozone sensitivity to the changes of precursors in urban atmosphere with in-situ observations of both VOCs and nitrogen oxides have been reported. Observation-based ozone chemical model, a useful tool to illustrate the ozone formation under different NO_x/VOCs conditions (Cardelino and Chameides, 1995, 2000; Zhang et al., 2007; Cheng et al., 2010), has been rarely applied to quantify ozone production in this region.

In order to get an in-depth and comprehensive understanding of the relationship between ozone production and its precursors in the YRD region and the roles of holiday effects and synoptic conditions, intensive campaign was conducted at the SORPES station, which is a regional background site of the YRD region (Ding et al., 2013a, 2016). The campaign covered the Chinese National Day holidays of 2014, when strong changes of human activities were expected, such as a reduced industrial production and increased traffic transportation. Meanwhile, anti-cyclone processes are quite typical in East Asia during this season. The anti-cyclones could provide favorable conditions of pollutant accumulation and the cold front tend to lead to the regional transport of pollutants (Ding et al., 2013a). The impacts of emission variation during the National Day holidays and the specific synoptic weather are addressed in this paper. In-situ observation of NO_x, carbon monoxide (CO), ozone, and VOCs combined with retroplume footprint analysis and an Observation based model (OBM) calculation based on the simplified MCM (master chemical mechanism) chemical mechanism CRI (Common Representative Intermediates) V2.1 (Jenkin et al., 2008) were applied in this work. The rest of this paper is structured as follows: Sect. 2 describes the site location and observation and modeling methodology. In Sect. 3, we analyze the VOC speciation, chemical reactivity, the ozone formation potential of different subgroups and its linkage with synoptic and holiday effects.

2. Field observations and modeling methodology

2.1. Observational station and instrumentation

The campaign was conducted at the SORPES station in Nanjing University Xianlin Campus, a suburban measurement site in the northeast to Nanjing downtown (118°′57′10″E, 32′°07′14″ N), during Sept. 22nd-Oct. 7th, 2014. The easterly prevailing wind and synoptic condition makes it a representative background site of Nanjing and a regional, downwind site of the city cluster in the YRD region (Ding et al., 2013a, 2016).

Online measurement with GC-MS/FID was conducted to obtain consistent VOC concentration with time resolution of 1 h, which included 5-min sampling period, 40-min analysis period and 8-min flush and cooling down. Short alkanes and alkenes (C2-C4) were separated with an Al_2O_3 PLOT column (DM-PLOT:30m × 0.32 mm i.d. × 3.0 μm) and quantified with a flame ionization detector (FID). Larger molecular VOCs (C5-C12 alkanes, alkenes, aromatic compounds, halides and oxygenated VOCs) were separated on a semi-polar column (DB624: 60M × 0.32 mm i.d. × 1.8 μm) and quantified with a quadruplet mass spectrometer (SHIMADZU QP2010-ULTRA). The initial column temperature of DM-PLOT and DB624 was set as 35 °C, kept for 3 min, raised to 180 °C with heating rate of 6 °C/min and then held for 5 min. Bromochloromethane, 1,4-difluorobenzene and 1-bromo-3-fluorobenzene were used as internal standards for MS calibration. Table S1 and Table S2 list the 97 VOC species that GC-FID and MS measured respectively.

Trace gases (O_3, sulfur dioxide (SO_2), NO, NO_x, total reactive nitrogen oxides (NO_y), and CO) at the SORPES station have been measured since 2011, with 90% data coverage and 1-min time resolution. Instruments (Thermo-fisher Scientific, TEI 49i, 43i 42i, 42i-Y and 48i) were auto span and zero checked with frequency of one week and one day, respectively, and manually calibrated once a week in case of the dis-function of auto calibration program. The TEI 42i was coupled with a highly selective photolytic converter to measure NO_2 (Xu et al., 2013). The 5-min averaging data were adopted considering both the capability of describing the concentration variation and proper signal noise ratio. Because of the high ozone concentration, daytime NO concentration appeared to be equivalent to the detection limit of NO detector used at the SORPES station. The NO detection limit was set to be 3 times of the standard deviation of the zero calibration data, which was around 0.5–1.2 ppb.

Meteorological measurements including relative humidity (RH), wind speed, wind direction, and air temperature were recorded by Automatic Weather Station (CAMPEEL co., AG1000). Consistent observations have been started since 2010. UVB total radiation was measured by UVB radiometer (UVS-B-T UV Radiometer, KIPP & ZONEN).

2.2. Modeling methodology

2.2.1. Lagrangian backward dispersion modeling

In order to diagnose the transport and dispersion characteristic of the air masses during the campaign, Lagrangian dispersion model was conducted by using Hybrid Single-Particle Lagrangian Integrated Trajectory (HYSPLIT) model (Stein et al., 2015). Briefly, for each hour during the study period, the model was run 2-day backwardly with 3 000 particles released every hour from the altitude of 100 m above the site. The model calculated the particle position with mean wind and turbulence transport component after being released at the receptor point. The residence time of particles below 100 m level was used to identify the "footprint"retroplume. The spatiotemporal distributions of these particles were used to evaluate the contribution from different regions to the pollutant transport. This method has been applied successfully to simulate transport of air pollution in eastern China and the Pearl River Delta region (Ding et al., 2013a,b). The reported results show that this method can well characterize the different transport processes of air pollution.

2.2.2. Observation-based chemical modeling

An observation-based chemical box model was used to investigate ozone chemistry and the sensitivity of ozone production to its precursors (Cardelino and Chameides, 1995, 2000; Cheng et al., 2010; Xue et al., 2013a). The model was based on a simplified MCM(CRI.2.1), a reduced mechanism describing ozone formation from the degradation of methane and 115 primary non-methane hydrocarbons and oxygenated volatile organic compounds, using the Master chemical Mechanism version 3.1(MCM v3.1) as a reference benchmark (Jenkin et al., 2008).

Before each simulation, the model was pre-run for seven days with constrains of observation data every hour, for the purpose that the unmeasured species would reach a steady state. The observed VOCs, other trace gases like CO, NO, NO_2, temperature, RH, UVB total radiation were used as inputs for model calculation in order to ensure that the simulation was under proper ratio of NOx and VOCs and real-time meteorology and radiation conditions. The measured real-time UVB radiation data was used to scale photochemical rate constant fitted from solar zenith angle under clear sky condition, which is calculated within the model (Saunders and Jenkin, 2003). For the NO data used in the model, all afternoon and low concentration NO data were set to be 1 ppb. The sensitivity of ozone concentration to the changes of ozone precursors (10% reduction) was investigated following the concept of Relative Incremental Reactivity (RIR), which is defined as the percent change of ozone photochemical production, with per percent change of one of its precursor or certain combination of some precursors (Carter and Atkinson, 1989). For RIR calculation, the model read VOCs, NO and CO concentrations every hour to constrain the simulation, and read air temperature, RH and scaled radiation every time step to calculate the kinetic rate constants.

2.2.3. Positive matrix factorization (PMF)

PMF was a well-developed and widely used receptor model in identifying sources in the atmosphere (Ling et al., 2011; Zhang et al., 2013; Yan et al., 2016). The principle was based on the work of Paatero and Tapper (1994). The advantage of PMF was that it can provide source profiles and contribution matrices without any prior knowledge and constrain the solutions to be non-negative. The measured 97 primary VOCs including alkanes, alkenes, aromatic compounds and halogenated hydrocarbons observed from Sept. 22nd – Oct. 7th were used as input of PMF. The uncertainties for each species were set to be 0.2 and the detect limit to be 0.015 ppb.

3. Results and discussion

3.1. VOC concentration and speciation

Table 1 shows the average concentration and variation of 30 most abundant VOCs measured during the campaign compared with results from previous study of Guangzhou and other 43 Chinese cities (Barletta et al., 2005; Liu et al., 2008a,b). The concentration of alkanes ranged from tens of ppt (part per trillion) to tens of ppb (part per billion) level with an average of 8.39 ppb, which was comparable with the range of previous studies. But the concentration level of alkenes and aromatic compounds was much lower compared with the result from Guangzhou. Moreover, the upper range of alkanes measured at the SORPES station exceeded the previous study from 43 Chinese cities. These differences might be attributed to different measurement method, site representativeness, and the chemical reactivity of different groups of VOCs. The VOC measurement conducted at Guangzhou and 43 Chinese cities was based on canister sampling at city sites and off-line analysis, while the observation conducted at the SORPES station was continuous on-line measurement. The direct emission of vehicle and other local sources near these measurement sites might be the reason for a higher concentration level of aromatic compounds and alkenes. The air parcel measured at the SORPES station was aged and well-mixed after passing through the city cluster. The low-reactivity species (alkanes, Benzene, etc.) accumulated and most of highly reactive species (Toluene, Propylene, etc.) were oxidized during transport. The off-line measurement at these city sites tended to overestimate the concentration levels of reactive species and underestimate the effect of low reactive but much more abundant species.

Fig. 1c and d shows the time series of total VOCs (tVOCs) measured at the SORPES site and the ratio of different subgroups to tVOCs. The measured 97 hydrocarbons are classified into 9 subgroups based on the structure of molecules and reactivity with OH radical, which are light alkanes ($C \leq 4$), long chain alkanes($C > 4$), short chain alkenes ($C \leq 4$), long alkenes ($C > 4$), BTEX (benzene, toluene, ethyl-benzene, xylene), other aro (other aromatic compounds), halides, alkyne and OVOCs. Halides, alkyne and short chain alkanes are low reactivity hydrocarbons, while alkenes, long chain alkanes, aromatic compounds (except benzene) and OVOCs are defined as reactive hydrocarbons (Zhang et al., 2007). The reason for grouping alkenes based on their molecular structure is that the two groups have different diurnal patterns. The separation of BETX out of other aro is because the majority of aromatic compounds is constituted of these four species. Short alkanes are the most dominant group of VOCs, followed by BTEX, long chain alkanes and halides. Such speciation agreed with other studies in China (Barletta et al., 2005). Moreover, we observed clear diurnal variation of alkenes. The concentration level of short alkenes was relatively low during daytime while increase dramatically during nighttime, indicating different chemical processes. Specifically, the reactions with OH radical and ozone is the main sink during daytime, while NO3 radical related reactions and ozonolysis take the place of the most dominant chemical processes during night (Arey and Atkinson, 2003; Atkinson, 1998; Carter, 2007). Inferred from high surface concentration of NO during nighttime (Fig. 1b), NO3 radical was barely present in the atmosphere and the rate

Table 1
The averaged mixing ratios (ppb) of VOCs measured by GC-FID/MS at the SORPES station and corresponding values in other studies.

Species	SORPES	SORPES	GZ[a]	43 cities[b]
	Range	Average ± std	Average ± std	Range
Ethane	1.04–9.36	2.65 ± 1.21	5.58 ± 3.34	3.7–17.0
Acetylene	0.30–7.32	1.56 ± 1.08	7.3 ± 5.2	2.9–58.3
Propane	0.23–9.87	1.48 ± 1.10	10.35 ± 8.53	1.5–20.8
n-Butane	0.15–18.22	1.42 ± 1.56	5.07 ± 4.42	0.6–14.5
Etylene	n.a.[c]-9.55	1.16 ± 1.51	6.55 ± 4.28	2.1–34.8
Iso-Pentane	0.08–23.79	1.11 ± 1.86	2.7 ± 2.3	0.3–18.8
Iso-Butane	0.12–11.02	0.90 ± 0.96	2.9 ± 2.6	0.4–4.6
n-Pentane	0.01–13.19	0.83 ± 1.28	1.19 ± 1.07	0.2–7.7
Benzene	0.15–4.44	0.72 ± 0.53	2.4 ± 1.9	0.7–10.4
Toluene	0.13–2.38	0.65 ± 0.41	7.0 ± 7.3	0.4–11.2
MEK	n.a.-3.37	0.53 ± 0.42		
Propylene	n.a. −10.03	0.36 ± 0.90	3.2 ± 3.0	
1,2-Dichloroethane	0.07–2.65	0.35 ± 0.24		
Acetone	0.12–2.27	0.30 ± 0.15		
Ethylbenzene	0.03–3.23	0.30 ± 0.32	1.16 ± 1.22	0.1–2.7
Chloromethane	n.a.-4.11	0.3 ± 0.34	1.18 ± 1.21	
2-Methylpentane	0.03–0.80	0.19 ± 0.13	1.03 ± 0.94	0.08–5.6
1,2-Dichloropropane	0.02–2.22	0.18 ± 0.24		0.2–10.1
m/p-Xylene	0.01–2.69	0.17 ± 0.23	1.46 ± 1.42	0.2–5.2
n-Hexane	0.02–0.91	0.17 ± 0.23	0.84 ± 0.80	
O-Xylene	0.01–1.26	0.13 ± 0.15	0.52 ± 0.5	0.1–6.9
1-Butene	n.a.-2.11	0.11 ± 0.22	1.33 ± 0.91	0.07–2.4
3-Methylpentane	0.01–0.90	0.10 ± 0.09	0.67 ± 0.64	0.1–3.6
2,3-Dimethylbutane	0.02–1.00	0.10 ± 0.10	0.26 ± 0.24	0.01–5.0
Isoprene	n.a.-0.82	0.09 ± 0.12	0.22 ± 0.17	0.04–1.7
Acetonitrile	0.01–0.30	0.09 ± 0.04	0.66 ± 0.29	
Carbon Terachloride	0.04–1.35	0.08 ± 0.10		
n-Dodecane	0.01–0.43	0.08 ± 0.10		
1-Pentene	n.a.-1.26	0.07 ± 0.12	0.18 ± 0.14	
Cis-1,1-Dichloroethene	n.a.-0.41	0.06 ± 0.07		
Trans-2-Butene	0.01–1.68	0.05 ± 0.08	0.4 ± 0.36	0.01–3.4
MTBE	n.a.-1.30	0.05 ± 0.05	0.96 ± 0.94	
cis-2-Butene	n.a.-0.47	0.01 ± 0.01	0.38 ± 0.33	0.02–3.7

[a] Data from (Barletta et al., 2005).
[b] Data from (Liu et al., 2008b).
[c] Under detection limit.

coefficient of alkenes with NO3 radical was much lower than that with OH radicals, which explained the high concentration of alkenes observed during night. One exception during the campaign was Sept. 23rd, 2014, considerable amount of ozone (~30 ppb) and almost no NO and short alkenes were observed during the night (Fig. 1b and c). Though no simultaneous measurement of radicals, we can infer from the ozone and NO concentration level that ozone and NO_3 radical are the important oxidants that consume alkenes during night. The observed Sept. 23rd case could support the assumption that the diurnal variation of short alkenes is related to different pathways of oxidation reactions.

Fig. 1a and b display the time series of meteorological parameters (air temperature, relative humidity, wind speed and wind direction), NO, NO_x, CO, O_3 and VOCs. It should be noted that the industry zone was located north to the station. Consequently, high VOC episodes appeared more frequent when north or northwest wind prevailed. Three types of episodes were defined during the measurement period. The first type was defined as fresh air mass, with high NO/NO_2 ratio and high CO concentration level. The second type was regional transport air mass, which was accompanied with high NO_2, but with almost near-zero NO concentration. During the third kind of episode, high NO/NO_2 ratio was observed but without obvious rise of CO concentration. This type of air mass was also freshly emitted but with different emission type, probably less combustion related (Streets et al., 2003). Ozone production efficiency (OPE = $\Delta O_x/\Delta NO_z$) during the campaign was diagnosed. The data chosen for OPE calculation was from 8:00 to 17:00 local time, during which period the photochemistry was strong. The OPE at SORPES was low (1.3–4.18) implying that Nanjing was in VOC-limited regime, which was consistent with that reported by Ding et al. (2013a). Compared with the OPE reported over China in the past decade (Wang et al., 2017), Nanjing was strongly VOC-limited with the lowest daily OPE to be 1.3 and the overall OPE to be 2.41.

During the campaign, alkanes was the most abundant group, followed by BTEX, alkyne, and short alkenes (only during night time).The averaged concentration of nighttime tVOCs was much higher than that during daytime, implying a substantial role of photochemical process in VOC consumption and dilution effect of boundary layer development. Moreover, the variation of CO correlated well with tVOCs variation, indicating CO and VOCs could have similar sources. NO_x concentration rose during the holiday (Oct. 1st-Oct. 7th), and the highest VOC concentration level during the campaign was observed on Oct 3rd. It may link to the holiday effects and the impact of VOCs and NO_x on ozone production will be discussed in the following section. Fig. 2 displays the diurnal variation of ozone, the total oxidants O_x (=O_3+ NO_2), NO_x(=NO + NO_2), and tVOCs. The diurnal variation of tVOCs has a negative correlation with the variation of O_x than with ozone, indicating that O_x is a better indicator of atmospheric oxidizing capacity than ozone. The validation of using CO-NO_y proxy to investigate the NO_x-VOC chemical mechanism is proved with VOCs observations, which correlated well with CO.

The ratio of ambient concentrations of VOCs with similar chemical reactivity equals to their ratio of original emission rate (Goldan et al., 2000; Jobson, 2004). When this theory is applied to real situations, complicated emission sources would obscure the

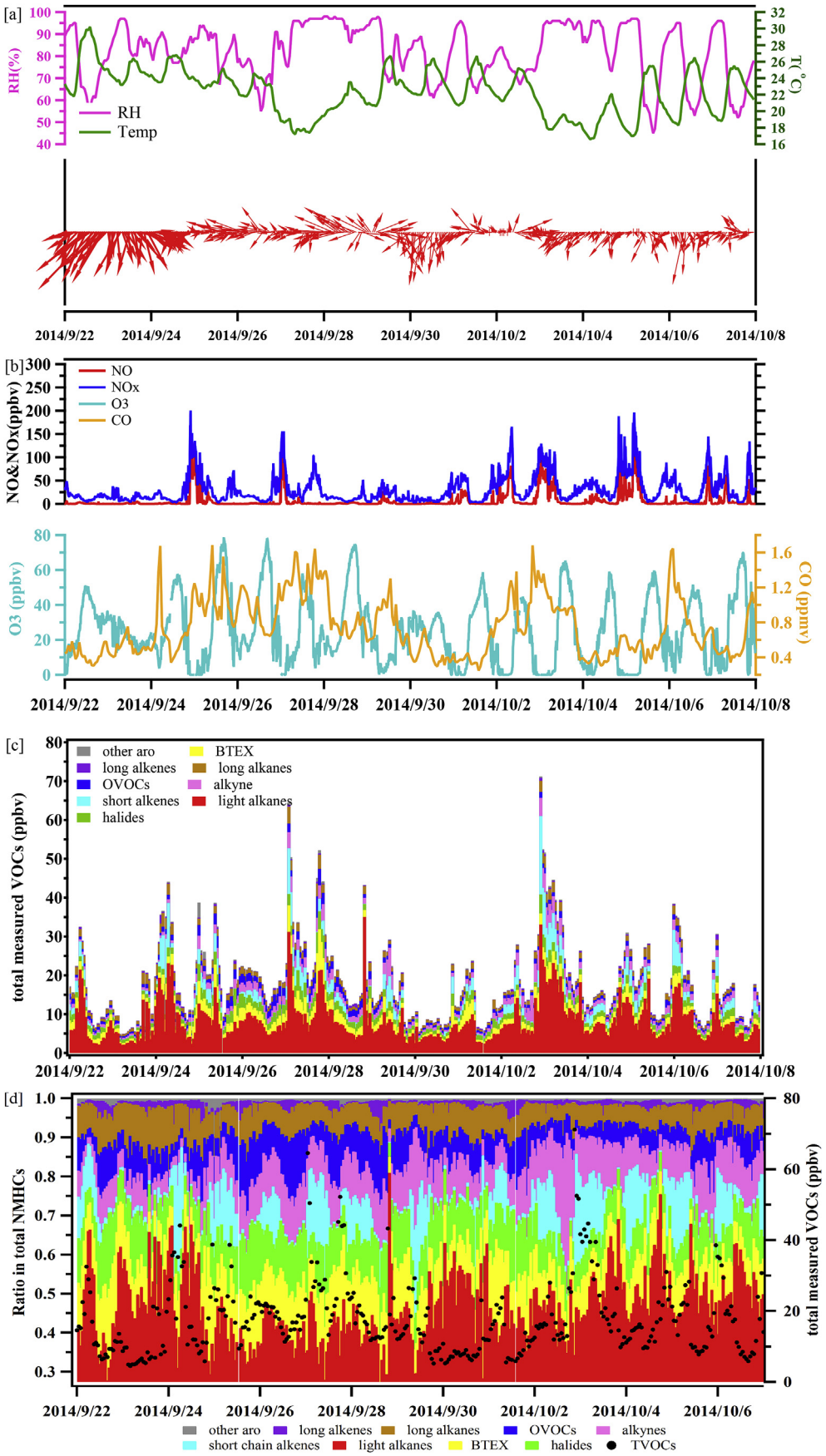

Fig. 1. The time series of [a] meteorology parameters (air temperature, RH, wind speed and direction), [b] trace gases (O3, CO, NO, and NO_x), [c] different groups of VOCs. [d] Hourly concentration of total VOCs (tVOCs, ppb) and the ratios of different VOC subgroups to tVOCs during the measurement period.

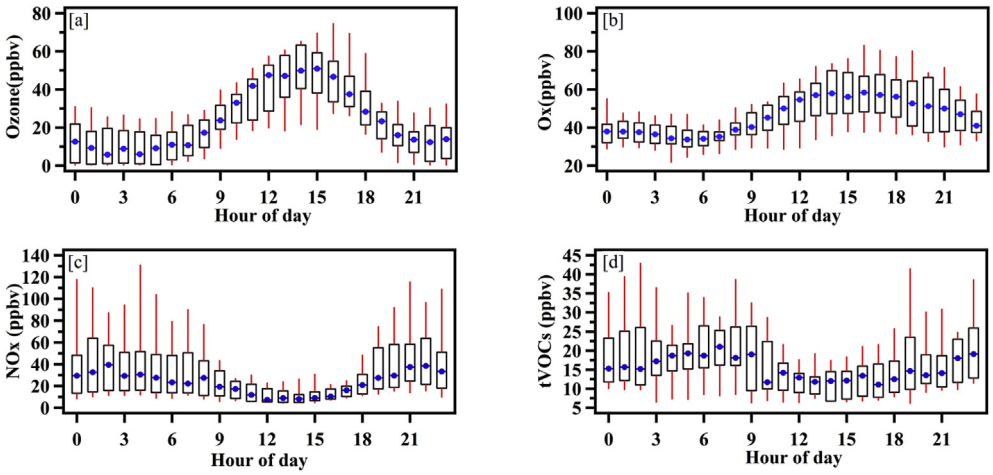

Fig. 2. Diurnal variations of [a]O_3, [b]O_x (O_3+ NO_2), [c]NO_x and [d]tVOCs. The dotted line represents median value, the upper and lower lines of box represent the 75th and 25th percentiles, respectively, and the upper and lower points of red lines represent the 90th and 10th percentiles. (For interpretation of the references to colour in this figure legend, the reader is referred to the web version of this article.)

inter-species comparison results. The combined use of photochemical age analysis would reveal more information about the source of specific VOCs.

The photochemical age of air masses was estimated by the ratio of observed toluene and benzene. The photochemical age was calculated using the method of de Gouw et al. (2005):

$$t = 1/[OH](k_{toluene}\text{-}k_{benzene}) \times [\ln([toluene]/[benzene]_{t=0})\text{-}ln([toluene]/[benzene])], \quad (1)$$

where [OH] is the 24-h averaged concentration of OH radicals (3.0×10^6 molecules cm^{-3}) (Warneke, 2004), and $k_{toluene}$ (5.63×10^{-12} cm^{-3} $molecule^{-1}$ s^{-1}) and $k_{benzene}$ (1.22×10^{-12} cm^{-3} $molecule^{-1}$ s^{-1}) are the rate coefficients for the reaction of OH with toluene and benzene (Arey and Atkinson, 2003). The emission ratio of toluene to benzene was calculated based on the linear fit of the canister sampling data from tunnel at Nanjing ($[toluene]/[benzene]_{t=0} = 3.16$). Fig. 3a shows the scatterplot of ethyl benzene ($k = 7.0 \times 10^{-12}$ $cm^{-3}molecule^{-1}$ s^{-1}) versus acetylene ($k = 1.22 \times 10^{-12}$ cm^{-3} $molecule^{-1}$ s^{-1}), colored by the photochemical age derived from equation (1). The slope of ethyl benzene/acetylene decreases with the increase of photochemical age. The rate constant of ethyl benzene is about six times larger than that of benzene which indicates that removal rate of ethyl benzene is much faster. The change of slope with photochemical age can be explained by their different reactivities, which indicates that the photochemical age derived from toluene and benzene ratio can, on some extent, describe the process of the removal of VOCs with different rate coefficients.

Benzene and acetylene have similar rate coefficient with OH radical, about 1.22×10^{-12} $cm^{-3}molecule^{-1}$ s^{-1}. Fig. 3b shows the scatterplot of benzene versus acetylene, also colored by the photochemical age. It shows a good correlation of benzene and acetylene with the correlation coefficient of 0.726 indicating that benzene and acetylene have similar sources. It is well acknowledged that acetylene is the product of incomplete combustion processes (Goldan et al., 2000; Liu et al., 2008b), while benzene is associated with vehicles emission (Wang et al., 2002), thus the source of benzene and acetylene is mainly related to fuel combustion of vehicular. The scatterplot also shows that the correlation of benzene and acetylene decreases with increase of photochemical age indicating the mixed air masses bring benzene from other sources such as industry emission and solvent evaporation. Figs. 3c and 4d display scatterplot of *n*-butane and *iso*-butane versus propane. Propane is the tracer of LPG evaporation and LPG powered vehicular emission (Liu et al., 2008a,b). A good correlation of both *n*-butane and *iso*-butane with propane was observed, with correlation coefficient of 0.796 and 0.804, respectively. The slop of *n*-butane and *iso*-butane versus propane was 1.212 and 0.75, respectively, different from the result from Guangzhou (0.48 and 0.28) (Liu et al., 2008b), and Mexico City (0.458 and 0.210) (Bravo and Sosa, 2002). The dispersed dots with longer photochemical age in Fig. 3c and d may be explained by long-range transport. The PMF results (Figs. S6–S8) resolved sources of LPG usage, which also indicated that propane, butanes and pentanes were the main constitutions of LPG related sources. Based on the diurnal variation of the contributions, we further distinguished traffic emissions with a clear two-peak shape corresponding to rush-hours. These results imply that LPG evaporation and LPG vehicular emission were important sources of light alkanes at the SORPES station. The different butane/propane ratio from previous studies suggests a different fuel usage in Nanjing. In fact, a program of use both natural gas and LPG to drive vehicles involving all taxis and part of private cars started since 2012. When vehicles drive with low speed, the fuel supply system would use natural gas instead. This would increase the evaporation of LPG.

To further understand the VOC sources, 6 factors were resolved for the VOC measurement during Sept. 22nd–Oct. 7th with PMF analysis. Because of short data span, the uncertainties of PMF results were inevitable. Factor profiles and contributions are shown in Figs. S6–S8. The factors were identified as LGD usage, traffic emission, biogenic emission, transported plume, PX-related industry and other industry. Factor 1 was dominated by acetylene, propane and n/i-butanes. Propane and butanes are traces of LDG (Blake and Rowland, 1995; Ling et al., 2011), and acetylene is the main constituents of internal combustion. Consequently, factor 1 was identified as LPG usage. Factor 2 was similar with Factor 1, but with much higher *i*/*n* pentane constitution. The diurnal variation of its contribution showed two peaks during rush hours. Therefore, Factor 2 was identified as traffic emission. Factor 3 showed a clear diurnal pattern with the contribution increased with the increase of temperature and solar radiation and was characterized by isoprene and its oxidant products (methyl vinyl ketone (MVK) and methacrolein (MACR)). Thus, Factor 3 was assigned to biogenic emissions. Factor 5 was characterized with mixed VOC groups including alkanes, OVOCs and aromatic compounds. The

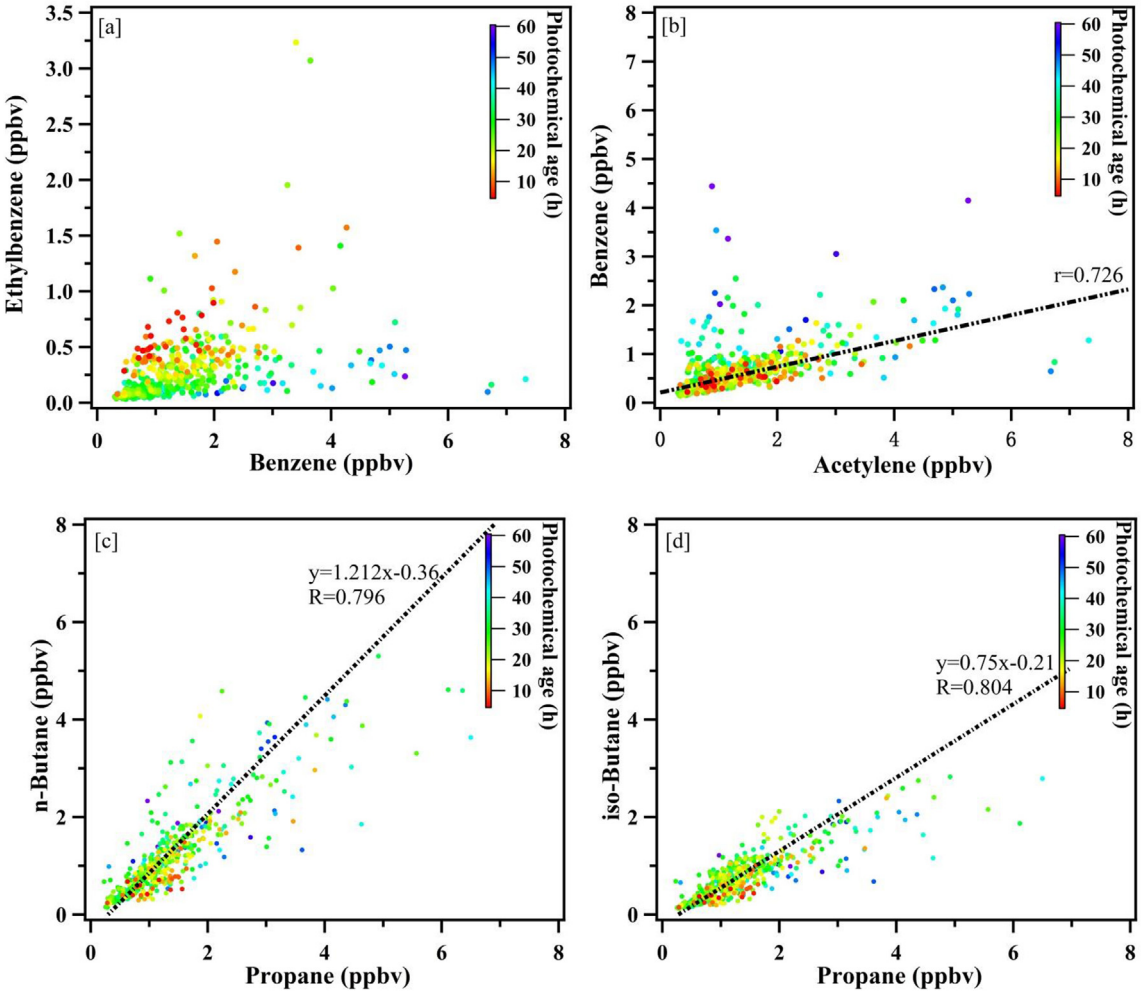

Fig. 3. Scatterplots of [a]acetylene versus ethyl benzene, [b]acetylene versus benzene, [c]propane versus n-butane and [d]propane versus *iso*-butane. The scatter points are colored by photochemical age derived from observed toluene/benzene ratio, based on equation (1).

contribution of this factor increased only during Sept. 25th–Sept. 29th. Thus, Factor 5 was characterized as transported plume based on the contribution time series. Factors 4 and 6 were defined as industry emissions because both of them had considerable fraction of benzene and toluene. The difference was that Factor 6 was also characterized with xylenes and the diurnal pattern indicated a stronger emission during nighttime. Since there is a p-Xylene (PX) chemical plant in Xianlin district, Factor 6 was further assigned as PX related industry.

3.2. Co-effect of synoptic condition and national holiday on VOCs

The distinct air masses transport characteristic and the holiday effect on the VOC speciation were observed during 2014 campaign.

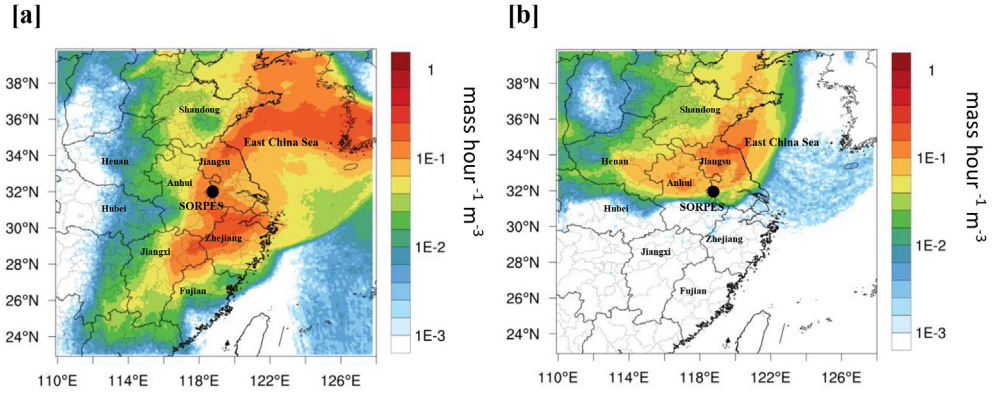

Fig. 4. Averaged retroplume (footprint residence time) of air parcels during working days [a] before the holiday, i.e. Sept. 24th- Sept. 30th and [b] during the National Day holidays of China, i.e. Oct. 1st- Oct. 7th.

Fig. 4 shows the averaged retroplume during working days before (Sept. 24th- Sept. 30th) and during the National Day holidays (Oct. 1st- Oct. 7th). Fig. 4a displays the average retroplume of Sept. 24th-Sept. 30th, the footprint shows two branches with one transport northeastward from south Japan, East China Sea and northern part of Jiangsu province, and another from adjacent southeastern provinces (Zhejiang, Fujian and Jiangxi). The average footprint distribution of Fig. 4a suggests a long footprint residence time over East China Sea and southeastern provinces of China. The clean air masses from the ocean and the low anthropogenic emission rate in southeast China (Fig. S1) leads to the relatively low concentration level of the observed NO and VOCs.

Fig. 4b shows the average retroplume of Oct. 1st-Oct. 7th, air masses mainly transported through northern part of Jiangsu province, Shandong province and adjacent Anhui and Henan provinces before arriving at the SORPES station. The effect of northern China was dominant, and the high footprint residence time reveals that the northern part of Jiangsu province is the region that contributes most to the observations during this period. The hourly mean footprint shows two anti-cyclone processes on Oct. 2nd and Oct. 5th, which transported air masses from northern region at a very fast speed. The development of these two anti-cyclones could be seen from the daily averaged retroplume of each day's transport characteristic in the support information (Fig. S1). The two anti-cyclones developed during Oct. 2nd-3rd and Oct. 5th-6th (Fig. S3), transporting air masses to the observational site from northern Jiangsu province and adjacent provinces. The first one was stronger, which brought air masses from nearly all Jiangsu and Anhui provinces and even from Henan and Shandong provinces, accompanied with sharp decrease of temperature, strong wind change and precipitation. The second one was much weaker that only northern Jiangsu province and Shandong province had a high footprint residence time, and the measurement site only experienced strong north wind. The accumulation of air pollutants during anti-cyclone was observed (Fig. 1). The tVOCs concentration increased sharply from 5.5 ppb to 71.2 ppb, and CO concentration increased from 0.33 ppm to 1.68 ppm, accompanied with strong wind shift from near static weather condition to more than 5 m/s and the highest daily temperature decrease from 26.7 to 19.6 Celsius degree. There was no much difference of NOx concentration during the anti-cyclone processes; the high NO/NOx ratio indicated that local emissions dominated the variation of NOx. These two convergent processes together with severe increase of traffic emission may play an important role in the ozone chemistry in the YRD region. When anti-cyclone weakened and vanished, the transport characteristic shifted to northeastward, which was quite typical during this season (Oct. 4th and 7th).

Significant increase of NO_y was observed during the National Day holidays (Fig. 5d) and the highest VOC concentration level during the campaign was observed on Oct. 3rd (Fig. 1). Since family vacation is a tradition during long holidays in China, we prefer to use transportation-related VOC species to estimate the holiday effect. As discussed above, acetylene measured at the SORPES station is mainly from vehicle emission and alkenes such as propene, ethylene and *iso*-/*n*-butene are the characteristic products of vehicles, thus acetylene and alkenes were chosen as tracers to estimate the human activity intensity. Fig. 5a shows diurnal variations of short alkenes/tVOCs ratio during the holidays and pre-holiday working days. Both periods show clear diurnal variations, alkene ratio kept deceasing from morning and were barely measured during the midday due to its high chemical activity. Compared with working days, during nighttime, the alkene ratio increased significantly, especially during 18:00–23:00 local time, corresponding to the variation of human activity. Fig. 5b uses acetylene as tracer to investigate the holiday effect. The diurnal variation of working days shows clearly the signal of morning rush hour around 06:00–10:00 local time. During national holiday, the acetylene ratio generally increased, and the obvious increase of acetylene ratio during 08:00–23:00 local time corresponded to the time of intensive human activities indicating an enhanced traffic emission. Figs. 5c and 6d demonstrate the diurnal variations of benzene/toluene ratio and NO_y before and during the holidays, respectively. The benzene/toluene ratio was applied to estimate the relative importance of traffic and industrial emissions as used in Liu et al. (2008b). During working days, the two peaks during rush hours (4:00–6:00, 18:00–22:00 local time) indicated that the benzene/toluene ratio could describe the variation of traffic emission. During the holiday, the ratio increase about 50%, compared with the value during working days. The higher benzene/toluene could be explained by enhanced vehicle emission and favorable convective condition during the holidays. Moreover, PMF analysis (Fig. S7) also showed an increase trend of LPG usage and traffic emissions at Oct. 3rd, 5th and 6th, consistent with high VOC episodes.

3.3. Chemical reactivity of VOCs and ozone production

The most important and direct process that increases ozone level in troposphere is the photolysis of NO_2 and O3 tends to be decreased by the titration reaction of NO with O_3. If sufficient NO_x is present in the atmosphere, which is the normal state in urban and suburban areas of China, the reactions of VOCs with atmospheric oxidants (mainly with OH radicals, if exist) forming peroxy radicals, which either consume NO or convert NO to NO_2, determine the ozone formation rate (Carter, 1994). OH (K_{OH}) reactivity is used here to estimate the initial formation rate of peroxy radical and to evaluate the chemical reactivity during different time of a day. This method is also used in previous studies (e.g. Liu et al., 2008b), which considers the first chemical step of full atmospheric chemistry with OH radical, and gives a general estimation of the contribution of this VOC species to atmospheric chemistry during daytime. K_{OH} is calculated by multiplying the OH reaction rate coefficient and the mixing ratio of the given compounds:

$$K_{OH} = [VOC]_i \times k_i^{OH}, \quad (2)$$

Where $[VOC]_i$ is the mixing ratio of the ith VOC compound and k_i^{OH} is the corresponding OH reaction rate coefficient. Here, the rate coefficients published by Arey and Atkinson (2003) were used in this work.

The same method is used on the nighttime data to estimate the relative contribution of each group of VOCs to the chemical reactivity during nighttime, using the chemistry reaction rate coefficient with NO_3radical (k_i^{NO3}) as a substitute to k_i^{OH}. It should be noted that though NO_3 radical is very important in the nighttime chemistry, only a few studies have reported the rate coefficient with alkenes, aromatic hydrocarbons, and oxygenated hydrocarbons. In this work we used NO_3 reaction rate coefficient with alkenes and aromatic hydrocarbons reported by Atkinson et al. (1984). In terms of aldehydes, values suggested by Cabañas et al. (2001) were applied.

Fig. 6 shows the averaged OH reactivity (during daytime) and NO_3 reactivity (during nighttime) of different groups of VOCs. Short chain alkenes contributed most to the chemical reactivity, followed by short alkanes and BTEX during morning, and the OH reactivity of short chain alkenes showed a peak during morning rush hours and gradually decreased during daytime, which might be explained by the diurnal variations of vehicular emissions. At rush hours, i.e. 07: 00–09: 00 and 16: 00–20: 00 local time, the increase of the chemical reactivity of alkanes (both short chain and long alkanes) and BTEX was also observed, indicating the effect of traffic emission

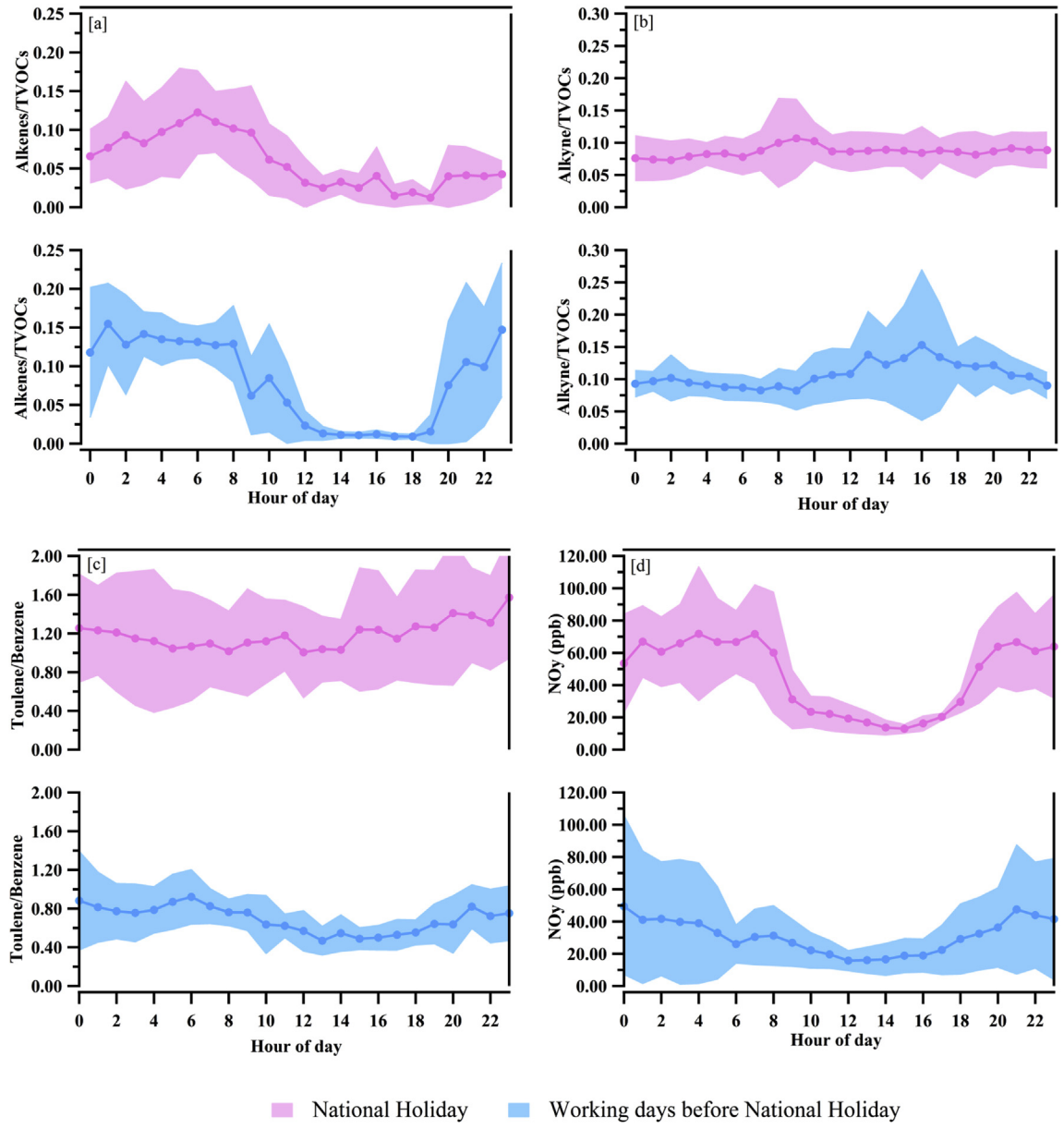

Fig. 5. Diurnal variations of [a] short alkenes versus total VOCs and [b] alkyne versus total VOCs during the National Day holidays of China and during workdays before the holidays. The filled area represents standard deviation.

on the total chemical reactivity of VOCs. NO_3 reactivity was used to estimate the chemical contribution during nighttime, since NO_3 radical reactions are important during nighttime in the troposphere (Atkinson, 1998). The NO_3 loss rate is about two factors smaller compared with OH loss rate, which could explain the diurnal variation of reactive alkenes (Fig. 1). Since the reactions with NO_3 radical are much slower, more short-chain alkenes could be observed during nighttime. Alkene-NO_3reactions were the dominant processes during nighttime, contributed to more than 90% of NO_3 reactivity, with the relative NO_3 reactivity of OVOCs and BTEX being less than 10% and 1%, respectively. Discrepancies of calculated OH reactivity and total OH reactivity have been reported from multiple studies, which might be related to the unmeasured and unidentified VOCs and the uncertainties of measurements (Yang et al., 2016). Unfortunately, there was no measurement of total OH reactivity during this campaign. However, the calculated OH reactivity and NO_3 reactivity does provide some information on contribution from specific VOC to the intensity of photochemistry. The variation of the OH reactivity of short chain alkenes indicated that the chemical processes after sunrise would be important. The accumulated reactive VOCs during night react with OH radical to produce considerable amount of peroxy radicals, which would not only enhance the ozone production but also secondary organic aerosol formation. Moreover, the NO_3 reactivity analysis during night time also revealed that short alkene reactions were the dominated processes. The night time reactions of alkenes with ozone and NO_3 radicals would be an important source of organic nitrate (Atkinson, 1998), especially in urban and suburban areas where the high concentration of alkenes was observed (Fig. 1) due to heavy traffic and industry load.

RIR was used as an index to assess the relative importance of the precursors to ozone production. The diagnosed RIRs of major cities during several ozone pollution episodes were studied by Xue et al. (2013b). The OBM results indicated that Shanghai and Guangzhou

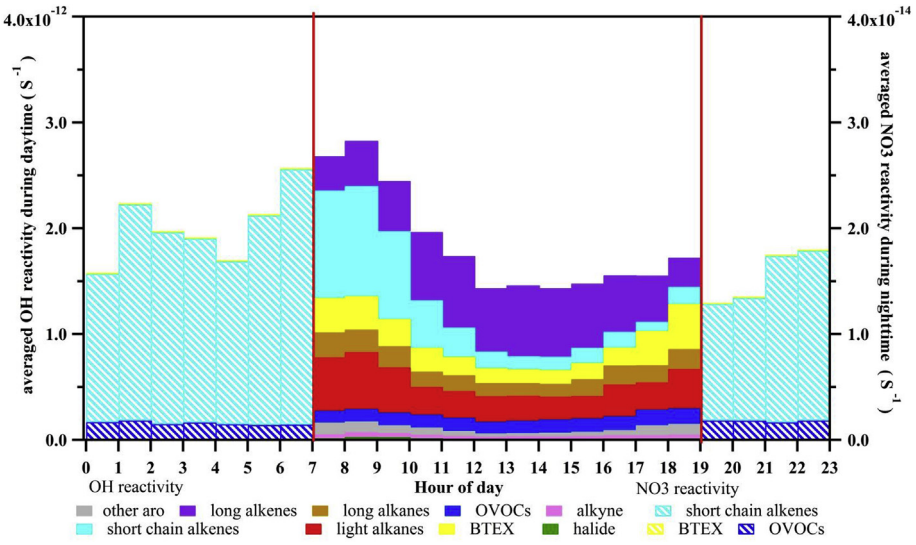

Fig. 6. Averaged OH/NO_3 reactivity of different groups of VOCs at the SORPES station. Note: the solid bars represent daytime OH reactivity and the dashed bars represent nighttime NO3 reactivity, respectively.

were VOC-limited regions with the dominant precursors to be aromatics and alkenes. Lanzhou, as an inland city with heavy petrochemical industry load, was a mixed regime, with alkenes, especially light olefins such as propene and ethene to be the most important VOC precursors. The RIRs diagnosed in Nanjing were consistent with the results in Shanghai.

The co-effect of synoptic condition and holiday effects on ozone production and the sensitivity of different precursors were discussed in this section. Fig. 7 shows the RIRs of major ozone precursors (upper panel) during the campaign and the RIRs of subgroups of VOCs (lower panel), which is categorized as reactive aromatic compounds (R-ARO), reactive olefins (R-OLE), alkanes which have more than 4 carbon atoms (C $\geq$ 4), and oxygenated VOCs (OVOCs). Generally, during the holiday the site was in VOC-Limited regime and the effect of CO cannot be neglected. The negative RIR value of NO suggested that the reduction of NO may cause the increase of ozone pollution in this area. While the control of both CO and VOCs emission would, in some extent, alleviate ozone issue. On Oct. 2nd, Oct. 5th and Oct. 6th when convergent process dominated, the RIR of CO increased compared with Oct. 1st and Oct. 7th when air masses were transported from northeast. The sensitivity test of the subgroups of AHC indicated that OVOC was the least important group contributed to ozone production. The other three subgroups competed to be the dominant precursor of ozone pollution under different synoptic conditions.

The simulated RIR results showed that on Sept. 30th, ozone

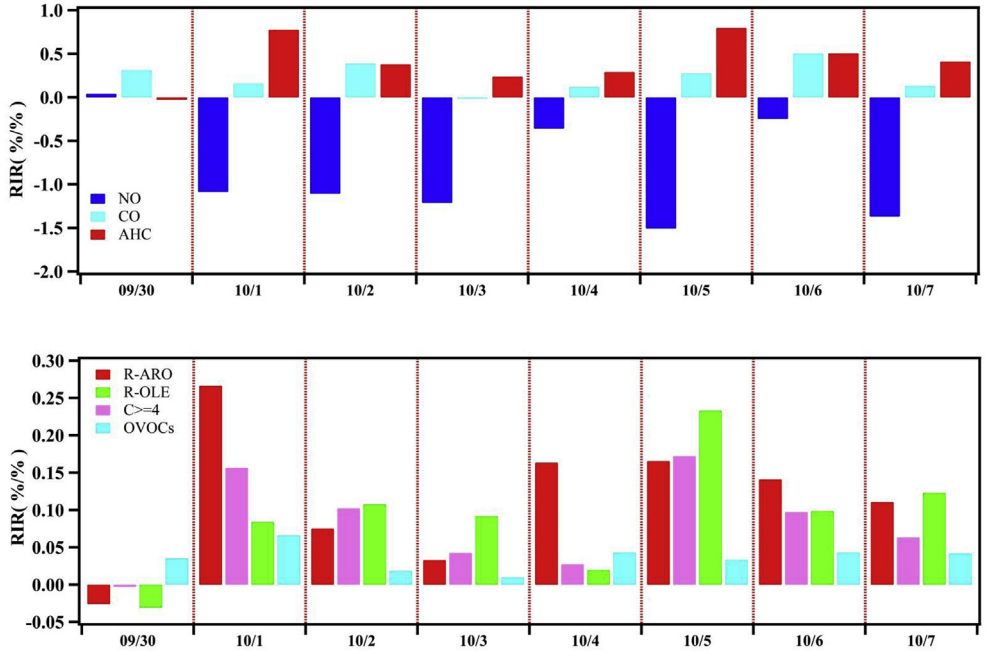

Fig. 7. OBM calculated RIRs for major precursors of ozone at SORPES. Note: The upper panel represents RIRs of NO, CO, and anthropogenic hydrocarbon compounds (AHC), the lower panel represents RIRs of the subgroups of AHC, R-ARO represents reactive aromatic compounds, R-OLE represents reactive olefins, C $\geq$ 4 represents alkanes which have more than 4 carbon atoms, and OVOCs represents oxygenated VOCs.

production rate was not sensitive to the reduction of its precursors (Fig. 7). The measurement data showed that on Sept. 30th the air mass was clean, with the lowest ozone concentration observed during the campaign (the ozone concentration was less than 40 ppb during the midday) and VOC concentration was also very low, with tVOCs concentration being less than 10 ppb and low active alkanes constituting more than half of the total amount. Furthermore, the UVB measurement showed that the radiation intensity was quite weak during the midday. The footprint of air mass suggested that the branch transported from the East China Sea and southeastern China was the dominant sources during the week before the holidays. The clean air mass and weak radiation might be the reason of low sensitivity of the precursors towards ozone formation.

During the National Day holidays, air mass mainly transported from North China, and anti-cyclone processes led to the accumulation of VOCs and other precursors. The RIR variation also reflected connections between transport and ozone production characteristics. On Oct. 2nd and Oct. 6th, during which time the anti-cyclone was most intensive, the effect of CO overweighed VOCs showing a non-neglectful effect of long-life species brought by regional transport (Fig. 7). The retroplume analysis indicated that the first anti-cyclone started and developed at Oct. 2nd, weakened and vanished at Oct. 3rd. The sharp increase of the RIR of CO was most likely attributed to the strong long-range transport. Similarly, the regional transport from north and northwest during Oct. 5th afternoon and Oct. 6th morning brings high concentration of CO, over 1.6 ppm, and the increasing RIR of CO from Oct. 4th to Oct. 6th was corresponded to the development of the anti-cyclone. On both cases, high CO concentration was observed during the night, the accumulated CO would react with OH radical during daytime to produce considerable amount of HO_2 radical, which would directly enhance the ozone production.

Along with the increase RIR of CO, the RIRs of VOC subgroups also changed with the development of anti-cyclone. On Oct. 1st and Oct. 4th air masses were transported from northeast, and the RIR results showed that aromatic compounds were the most important precursors that led to ozone production in these two days which was consistent with the simulation results (Tie et al., 2013; Zhang et al., 2015). During Oct. 2nd −Oct. 3rd and Oct. 5th −Oct. 6th, when two strong regional transport processes from north and northwest were observed, the different RIR distributions of VOC subgroups were found to be in consistent with the change of transport pattern. RIR of both cases showed significant increase of alkanes and alkenes compared with Oct. 1st and Oct. 4th, and alkenes became the most dominant precursors of ozone production. As showed in Fig. 5, during the holidays the traffic emission was strongly enhanced. The co-effect of enhanced human activities and suitable synoptic weather condition made alkenes the most sensitive precursor towards ozone formation, and the role of alkanes, which were also related to motor vehicle emission, was also enhanced. During Oct. 6th, the effect of alkanes even overweighed aromatics compounds, indicating that under strong regional transport condition, the effects of low reactive VOC species were also important.

The low RIR of both VOC and CO on Oct. 3rd could be explained by the weather condition. The high RH of whole day and weak diurnal variation of temperature (Fig. 1) indicated that precipitation during daytime hindered the photochemical processes, and titration effect led to the high negative RIR of NO.

4. Conclusions

For the purpose of understanding the influence of synoptic condition and holiday effects on ozone production in the Yangtze River Delta region, concentrations of speciated volatile organic compounds (VOCs) and ozone were simultaneously measured at the Station for Observing Regional Processes of the Earth System (SORPES) around the National Day holidays of 2014. When compared with canister samples and off-line measurements from other studies, here we observed high alkanes and less aromatics compounds and alkenes, which was related to the chemical reactivity and the age of air mass. Clear diurnal variations of short alkenes were observed, high concentration level of short alkenes could only be observed during the night and the boundary layer effect was excluded by the diurnal variations of the ratio of subgroups to total VOCs. This diurnal variation of short chain alkenes could be attributed to the relatively low reaction rate coefficient with NO_3 radical during nighttime.

The inter-species comparison coupled with photochemical age derived from toluene/benzene ratio indicated that benzene and acetylene were related to vehicle emissions, while benzene had other sources, such as industry emissions and solvent usage. The results also showed that LPG usage was the main sources of propane and butane and other short chain alkanes. Among all the species, short alkenes were the most important subgroup of VOCs during nighttime and contributed to more than 90% of chemical reactivity, while during daytime clear signal of rush hour were observed from VOC chemical reactivity.

Relative Incremental Reactivity (RIR) was calculated based on OBM, and the co-effects of synoptic condition and holiday effects were investigated. Acetylene, short alkenes and Toluene/Benzene ratio were used as tracers of traffic emissions to investigate the holiday effect during national holiday. Strong signals of human activity during “non-sleep” hours were observed compared with working days. Meanwhile, pollutant accumulation was observed during anti-cyclone processes: The tVOCs concentration increased from 5.5 ppb to 71.2 ppb, and CO concentration increased from 0.33 ppm to 1.68 ppm. The relative contributions of CO, NO and subgroups of VOCs to ozone production were estimated with OBM. When industrial emission dominated, corresponding to the northeastward retroplume, aromatic compounds were the most important precursors of ozone production. When air masses shifted to a more regional transport pattern under the effect of anti-cyclone processes, the co-effect of intensive human activities during national holidays and regional transport of the air pollutants from north and northwest of Nanjing led to a significant enhancement role of CO, alkenes and alkanes on ozone production.

Acknowledgments

The work was supported by Jiangsu Provincial Science Fund (BK20140021, BK20160620), Jiangsu provincial environmental monitoring fund (1410), Ministry of Science and Technology of the People's Republic of China (2016YFC0200506, 2016YFC0202002), NSFC (D0512/41422504, D0512/91544231) and National Key Technology Research and Development Program (2014BAC22B02). We thank Y.C. Shen, Y.N. Xie for their contributions to field measurement and instrumentation maintenance.

Appendix A. Supplementary data

Supplementary data related to this article can be found at http://dx.doi.org/10.1016/j.atmosenv.2017.08.035.

References

Arey, J., Atkinson, R., 2003. Atmospheric degradation of volatile organic compounds. Chem. Rev. 103, 4605–4638.
Atkinson, R., 1998. Atmospheric chemistry of VOCs and NOx. Atmos. Environ. 34 (2000), 2063–2101.
Atkinson, R., Plum, C.N., Carter, W.P.L., Winer, A.M., Pitts, J.N., 1984. Jr., Rate

constants for the gas-phase reactions of nitrate radicals with a series ofOrganics in air at 298 ±1 K. J. Phys. Chem. 88, 1210–1215.
Barletta, B., Meinardi, S., Sherwood Rowland, F., Chan, C.Y., Wang, X., Zou, S., Yin Chan, L., Blake, D.R., 2005. Volatile organic compounds in 43 Chinese cities. Atmos. Environ. 39 (32), 5979–5990.
Blake, D.R., Rowland, F.S., 1995. Urban leakage of liquefied petroleum gas and its impact on Mexico City air quality. Science 269, 953–956.
Bravo, H., Sosa, R., 2002. Concentrations of benzene and toluene in the atmosphere of the southwestern area at tha Mexico City Metropolitan Zone. Atmos. Environ. 36, 3843–3849.
Brönnimann, S., Neu, U., 1997. Weekend-Weekday differences of near-surface ozone concentrations in Switzerland for different meterological conditions. Atmos. Environ. 31 (8), 1127–1135.
Brunekreef, B., Holgate, S.T., 2002. Air pollution and health. Lancet 360 (9341), 1233–1242.
Cabañas, B., Martin, P., Salgado, S., Ballesteros, B., Martínez, E., 2001. An experimental study on the temperature dependence for the gas-phase reactions of NO_3 radical with a series of aliphatic aldehydes. J. Atmos. Chem. 40, 23–39.
Cardelino, C.A., Chameides, W.L., 1995. An observation-based model for analyzing ozone precursor relationships in the urban atmosphere. J. Air & Waste Manag. Assoc. 45 (3), 161–180.
Cardelino, C.A., Chameides, W.L., 2000. The application of data from photochemical assessment monitoring stations to the observation-based model. Atmos. Environ. 34, 2325–2332.
Carter, W.P.L., 1994. Development of ozone reactivity scales for volatile organic compounds. J. Air Waste Manag. Assoc. 44, 881–899.
Carter, W.P.L., 2007. A detailed mechanism for the gas-phase atmospheric reactions of organic compounds. Atmos. Environ. 41, 80–117.
Carter, W.P.L., Atkinson, R., 1989. Computer modeling study of incremental hydrocarbon reactivity. Environ. Sci. Technol. 23, 864–880.
Chameides, W.L., 1992. Ozone precursor relationships in the ambient atmosphere. J. Geophys. Res. 97 (D5), 6037–6055.
Cheng, R., Guo, H., Wang, X., Saunders, S.M., Lam, S.H.M., Jiang, F., Wang, T., Ding, A., Lee, S., Ho, K.F., 2010. On the relationship between ozone and its precursors in the Pearl River Delta: application of an observation-based model (OBM). Environ. Sci. Pollut. Res. 17 (3), 547–560.
de Gouw, J.A., Middlebrook, A.M., Warneke, C., Goldan, P.D., Kuster, W.C., Roberts, J.M., Fehsenfeld, F.C., Worsnop, D.R., Canagaratna, M.R., Pszenny, A.A.P., Keene, W.C., Marchewka, M., Bertman, S.B., Bates, T.S., 2005. Budget of organic carbon in a polluted atmosphere: results from the New england air quality study in 2002. J. Geophys. Res. 110 (D16).
Ding, A.J., Wang, T., Zhao, M., Wang, T., Li, Z., 2004. Simulation of sea-land breezes and a discussion of their implications on the transport of air pollution during a multi-day ozone episode in the Pearl River Delta of China. Atmos. Environ. 38 (39), 6737–6750.
Ding, A.J., Wang, T., Xue, L., Gao, J., Stohl, A., Lei, H., Jin, D., Ren, Y., Wang, X., Wei, X., Qi, Y., Liu, J., Zhang, X., 2009. Transport of north China air pollution by mid-latitude cyclones: case study of aircraft measurements in summer 2007. J. Geophys. Res. 114 (D8).
Ding, A.J., Fu, C.B., Yang, X.Q., Sun, J.N., Zheng, L.F., Xie, Y.N., Herrmann, E., Nie, W., Petäjä, T., Kerminen, V.M., Kulmala, M., 2013a. Ozone and fine particle in the western Yangtze River Delta: an overview of 1 yr data at the SORPES station. Atmos. Chem. Phys. 13 (11), 5813–5830.
Ding, A.J., Wang, T., Fu, C., 2013b. Transport characteristics and origins of carbon monoxide and ozone in Hong Kong, South China. J. Geophys. Res. Atmos. 118 (16), 9475–9488.
Ding, A.J., Nie, W., Huang, X., Chi, X.G., Sun, J., Kerminen, V., Xu, Z., Guo, W., Petäjä, T., Yang, X., Kulmala, M., Fu, C., 2016. Long-term observation of air pollution-weather/climate interactions at the SORPES station: a review and outlook. Front. Environ. Sci. Eng. 10 (5).
Ding, A.J., Huang, X., Fu, C., 2017a. Air Pollution and Weather Interaction in East Asia, Oxford Research Encyclopedia of Environmental Science. http://dx.doi.org/10.1093/acrefore/9780199389414.013.536.
Ding, A.J., et al., 2017b. Ozone in the western Yangtze River Delta of China: a synthesis study based on ground, aircraft and sounding measurements in Nanjing, 2011-2017. Atmos. Chem. Phys. (in preparation).
Fuhrer, J., Skarby, L., Ashmore, M.R., 1997. Critical levels for ozone effects on vegetation in Europe. Environ. Pollut. 97 (1–2), 91–106.
Goldan, P.D., Parrish, D.D., Kuster, W.C., Trainer, M., McKeen, S.A., Holloway, J., Jobson, B.T., Sueper, D.T., Fehsenfeld, F.C., 2000. Airborne measurements of isoprene, CO, and anthropogenic hydrocarbons and their implications. J. Geophys. Res. Atmos. 105 (D7), 9091–9105.
Guo, H., Jiang, F., Cheng, H.R., Simpson, I.J., Wang, X.M., Ding, A.J., Wang, T.J., Saunders, S.M., Wang, T., Lam, S.H.M., Blake, D.R., Zhang, Y.L., Xie, M., 2009. Concurrent observations of air pollutants at two sites in the Pearl River Delta and the implication of regional transport. Atmos. Chem. Phys. 9 (19), 7343–7360.
Huang, C., Chen, C.H., Li, L., Cheng, Z., Wang, H.L., Huang, H.Y., Streets, D.G., Wang, Y.J., Zhang, G.F., Chen, Y.R., 2011. Emission inventory of anthropogenic air pollutants and VOC species in the Yangtze River Delta region, China. Atmos. Chem. Phys. 11 (9), 4105–4120.
Intergovernmental Panel on Climate Change(IPCC), 2013. Climate change 2013: the physical science basis. In: Stocker, T.F., Qin, D., Plattner, G.-K., Tignor, M., Allen, S.K., Boschung, J., Midgley, P.M. (Eds.), Contribution of Working Group I to the Fifth Assessment Report of the Intergovernmental Panel on Climate Change. Cambridge University Press, Cambridge, U.K., and New York.
Jenkin, M.E., Watson, L.A., Utembe, S.R., Shallcross, D.E., 2008. A Common Representative Intermediates (CRI) mechanism for VOC degradation. Part 1: gas phase mechanism development. Atmos. Environ. 42 (31), 7185–7195.
Jiang, F., Zhou, P., Liu, Q., Wang, T., Zhuang, B., Wang, X., 2012. Modeling tropospheric ozone formation over East China in springtime. J. Atmos. Chem. 69 (4), 303–319.
Jobson, B.T., 2004. Hydrocarbon source signatures in Houston, Texas: influence of the petrochemical industry. J. Geophys. Res. 109 (D24).
Levy, I., 2013. A national day with near zero emissions and its effect on primary and secondary pollutants. Atmos. Environ. 77, 202–212.
Li, L., An, J.Y., Shi, Y.Y., Zhou, M., Yan, R.S., Huang, C., Wang, H.L., Lou, S.R., Wang, Q., Lu, Q., Wu, J., 2016. Source apportionment of surface ozone in the Yangtze River Delta, China in the summer of 2013. Atmos. Environ. 144, 194–207.
Ling, Z., Guo, H., Cheng, H.R., Yu, Y.F., 2011. Sources of ambient volatile organic compounds and their contributions to photochemical ozone formation at a site in the Pearl River Delta, southern China. Environ. Pollut. 159 (10), 2310–2319.
Liu, Y., Shao, M., Fu, L., Lu, S., Zeng, L., Tang, D., 2008a. Source profiles of volatile organic compounds (VOCs) measured in China: Part I. Atmos. Environ. 42 (25), 6247–6260.
Liu, Y., Shao, M., Lu, S., 2008b. Volatile organic compound(VOC) measurements in the Pearl River Delta (PRD) region, China. Atmos. Chem. Phys. 8, 1531–1545.
Paatero, P., Tapper, U., 1994. Positive matrix factorization: a non-negative factor model with optimal utilization of error estimates of data values. Environmetrics 5, 111–126.
Pollack, I.B., Ryerson, T.B., Trainer, M., Parrish, D.D., Andrews, A.E., Atlas, E.L., Blake, D.R., Brown, S.S., Commane, R., Daube, B.C., de Gouw, J.A., Dubé, W.P., Flynn, J., Frost, G.J., Gilman, J.B., Grossberg, N., Holloway, J.S., Kofler, J., Kort, E.A., Kuster, W.C., Lang, P.M., Lefer, B., Lueb, R.A., Neuman, J.A., Nowak, J.B., Novelli, P.C., Peischl, J., Perring, A.E., Roberts, J.M., Santoni, G., Schwarz, J.P., Spackman, J.R., Wagner, N.L., Warneke, C., Washenfelder, R.A., Wofsy, S.C., Xiang, B., 2012. Airborne and ground-based observations of a weekend effect in ozone, precursors, and oxidation products in the California South Coast Air Basin. J. Geophys. Res. Atmos. 117 (D21).
Saunders, S.M., Jenkin, M.E., 2003. Protocol for the development of the Master Chemical Mechanism, MCM v3(Part A): tropospheric degradation of non-aromatic volatile organic compounds. Atmos. Chem. Phys. 3, 161–180.
Seinfeld, J.H., Pandis, S.N., 2006. Atmospheric Chemistry and Physics. John Wiley, Hoboken, N. J.
Shao, M., Zhang, Y., Zeng, L., Tang, X., Zhang, J., Zhong, L., Wang, B., 2009. Ground-level ozone in the Pearl River Delta and the roles of VOC and NOx in its production. J. Environ. Manag. 90 (1)), 512–518.
Stein, A.F., Draxler, R.R., Rolph, G.D., Stunder, B.J.B., Cohen, M.D., Ngan, F., 2015. NOAA's HYSPLIT atmospheric transport and dispersion modeling system. Bull. Am. Meteorol. Soc. 96 (12), 2059–2077.
Streets, D.G., Bond, T.C., Carmichael, G.R., Fernandes, S.D., Fu, Q., He, D., Klimont, Z., Nelson, S.M., Tsai, N.Y., Wang, M.Q., Woo, J.H., Yarber, K.F., 2003. An inventory of gaseous and primary aerosol emissions in Asia in the year 2000. J. Geophys. Res. Atmos. 108 (D21).
Tan, P.H., Chou, C., Liang, J.Y., Chou Charles, C.K., Shiu, C.J., 2009. Air pollution "holiday effect" resulting from the Chinese New Year. Atmos. Environ. 43 (13), 2114–2124.
Tan, P.H., Chou, C., Chou Charles, C.K., 2013. Impact of urbanization on the air pollution "holiday effect" in Taiwan. Atmos. Environ. 70, 361–375.
Tie, X., Geng, F., Guenther, A., Cao, J., Greenberg, J., Zhang, R., Apel, E., Li, G., Weinheimer, A., Chen, J., Cai, C., 2013. Megacity impacts on regional ozone formation: observations and WRF-Chem modeling for the MIRAGE-Shanghai field campaign. Atmos. Chem. Phys. 13 (11), 5655–5669.
Wang, X.M., Sheng, G.Y., Fu, J.M., 2002. Urban roadside aromatic hydrocarbons in three cities of the Pearl River Delta, People's Republic of China. Atmos. Environ. 36, 5141–5148.
Wang, X.M., Chen, F., Wu, Z.Y., 2009. Impacts of weather conditions Modified by urban expansion on surface ozone: comparison between the Pearl River Delta and Yangtze River dleta regions. Adv. Atmos. Sci. 26 (5), 962–972.
Wang, T., Xue, L., Brimblecombe, P., Lam, Y.F., Li, L., Zhang, L., 2017. Ozone pollution in China: a review of concentrations, meteorological influences, chemical precursors, and effects. Sci. Total Environ. 575, 1582–1596.
Warneke, C., 2004. Comparison of daytime and nighttime oxidation of biogenic and anthropogenic VOCs along the New england coast in summer during New england air quality study 2002. J. Geophys. Res. 109 (D10).
Wei, X.L., Lam, K.S., Cao, C., Li, H., He, J., 2016. Dynamics of the Typhoon Haitang related high ozone episode over Hong Kong. Adv. Meteorol. 2016, 6089154.
Xie, M., Zhu, K., Wang, T., Chen, P., Han, Y., Li, S., Zhuang, B., Shu, L., 2016. Temporal characterization and regional contribution to O3 and NOx at an urban and a suburban site in Nanjing, China. Sci. Total Environ. 551–552, 533–545.
Xu, Z., Wang, T., Xue, L.K., Louie Peter, K.K., Luk Connie, W.Y., Gao, J., Wang, S.L., Chai, F.H., Wang, W.X., 2013. Evaluating the uncertainties of thermal catalytic conversion in measuring atmospheric nitrogen dioxide at four differently polluted sites in China. Atmos. Environ. 76, 221–226.
Xue, L.K., Wang, T., Guo, H., Blake, D.R., Tang, J., Zhang, X.C., Saunders, S.M., Wang, W.X., 2013a. Sources and photochemistry of volatile organic compounds in the remote atmosphere of western China: results from the Mt. Waliguan Observatory. Atmos. Chem. Phys. 13 (17), 8551–8567.
Xue, L.K., Wang, T., Gao, J., Ding, A.J., Zhou, X.H., Blake, D.R., Wang, X.F., Saunders, S.M., Fan, S.J., Zuo, H.C., Zhang, Q.Z., Wang, W.X., 2013b. Ozone

production in four major cities of China: sensitivity to ozone precursors and heterogeneous processes. Atmos. Chem. Phys. 13 (10), 27243–27285.
Xue, L.K., Wang, T., Gao, J., Ding, A.J., Zhou, X.H., Blake, D.R., Wang, X.F., Saunders, S.M., Fan, S.J., Zuo, H.C., Zhang, Q.Z., Wang, W.X., 2014. Ground-level ozone in four Chinese cities: precursors, regional transport and heterogeneous processes. Atmos. Chem. Phys. 14 (23), 13175–13188.
Yan, C., Nie, W., Äijälä, M., Rissanen, M.P., Canagaratna, M.R., Massoli, P., Junninen, H., Jokinen, T., Sarnela, N., Häme, S.A.K., Schobesberger, S., Canonaco, F., Yao, L., Prévôt, A.S.H., Petäjä, T., Kulmala, M., Sipilä, M., Worsnop, D.R., Ehn, M., 2016. Source characterization of highly oxidized multifunctional compounds in a boreal forest environment using positive matrix factorization. Atmos. Chem. Phys. 16 (19), 12715–12731.
Yang, Y., Shao, M., Wang, X., Nölscher, A.C., Kessel, S., Guenther, A., Williams, J., 2016. Towards a quantitative understanding of total OH reactivity: a review. Atmos. Environ. 134, 147–161.
Zhang, J., Wang, T., Chameides, W.L., Cardelino, C., Kwok, J., Blake, D.R., Ding, A., So, K.L., 2007. Ozone production and hydrocarbon reactivity in Hong Kong, Southern China. Atmos. Chem. Phys. 7, 557–573.
Zhang, Y.H., Hu, M., Zhong, L.J., Wiedensohler, A., Liu, S.C., Andreae, M.O., Wang, W., Fan, S.J., 2008. Regional integrated experiments on air quality over Pearl River Delta 2004 (PRIDE-PRD2004): overview. Atmos. Environ. 42 (25), 6157–6173.
Zhang, Y., Mao, H., Ding, A., Zhou, D., Fu, C., 2013. Impact of synoptic weather patterns on spatio-temporal variation in surface O3 levels in Hong Kong during 1999-2011. Atmos. Environ. 73, 41–50.
Zhang, L., Zhu, B., Gao, J., 2015. Modeling Study of A Typical summer ozone pollution event over Yangtze River Delta. Environ. Sci. 36 (11), 3981–3988.

Further reading

Chan, L.Y., Chu, K.W., Zou, S.C., Chan, C.Y., Wang, X.M., Barletta, B., Blake, D.R., Guo, H., Tsai, W.-Y., 2006. Characteristics of nonmethane hydrocarbons (NMHCs) in industrial, industrial-urban, and industrial-suburban atmospheres of the Pearl River Delta (PRD) region of south China. J. Geophys. Res. 111 (D11).
Derwent, R.G., Jenkin, M.E., Saunders, S.M., Pilling, M.J., Simmonds, P.G., Passant, N.R., Dollard, G.J., Dumitrean, P., Kent, A., 2003. Photochemical ozone formation in north west Europe and its control. Atmos. Environ. 37 (14), 1983–1991.
Mckeen, S.A., Liu, S.C., 1993. Hydrocarbon ratios and photochemical history of air masses. Geophys. Res. Lett. 20 (21), 2363–2366.
Na, K., Kim, Y.P., Moon, K.C., 2003. Diurnal characteristics of volatile organic compounds in the Seoul atmosphere. Atmos. Environ. 37 (6), 733–742.
Ran, L., Zhao, C., Geng, F., Tie, X., Tang, X., Peng, L., Zhou, G., Yu, Q., Xu, J., Guenther, A., 2009. Ozone photochemical production in urban Shanghai, China: analysis based on ground level observations. J. Geophys. Res. 114 (D15).
Ryerson, T.B., 2003. Effect of petrochemical industrial emissions of reactive alkenes and NO_x on tropospheric ozone formation in Houston, Texas. J. Geophys. Res. 108 (D8).